

Influence of octupole vibration on the low-lying structure of ^{251}Fm and other heavy $N = 151$ isotones

K. Rezyunkina,^{1,2,*} A. Lopez-Martens,¹ K. Hauschild,¹ I. Deloncle,¹ S. Péru,³ P. Brionnet,⁴ M. L. Chelnokov,⁵ V. I. Chepigin,⁵ O. Dorvaux,⁴ F. Déchery,⁴ H. Faure,⁴ B. Gall,⁴ A. V. Isaev,⁵ I. N. Izosimov,⁵ D. E. Katrsev,⁵ A. N. Kuznetsov,⁵ A. A. Kuznetsova,⁵ O. N. Malyshev,⁵ A. G. Popeko,⁵ Y. A. Popov,⁵ E. A. Sokol,⁵ A. I. Svirikhin,⁵ and A. V. Yeremin⁵

¹CSNSM, Univ. Paris-Sud, CNRS/IN2P3, Université Paris-Saclay, 91405 Orsay, France

²KU Leuven, Instituut voor Kern- en Stralingsfysica, B-3001 Leuven, Belgium

³CEA/DAM-Ile-de-France, Service de Physique Nucléaire, Bruyères-le-Châtel, F-91297 Arpajon Cedex, France

⁴IPHC-DRS/Université de Strasbourg, IN2P3-CNRS, UMR 7178, F-67037 Strasbourg, France

⁵FLNR, JINR, 141980 Dubna, Russia



(Received 6 March 2018; published 31 May 2018)

The structure of low-lying excited states in ^{251}Fm , populated by the α decay of ^{255}No , has been investigated by means of combined γ and internal conversion electron spectroscopy. The values for the internal conversion coefficients for the $1/2^+ \rightarrow 5/2^+$ and $5/2^+ \rightarrow 9/2^-$ transitions have been measured. The determined $M2/E3$ mixing ratio and lifetime for the $5/2^+$ decay to the ground state allowed to determine the corresponding reduced transitions strengths of $B(E3) = 18(6)$ W.u. and $B(M2) = 3.0(6) \times 10^{-3}$ W.u. These results, as well as the results of previous studies in $N = 151$ isotopes, are compared to theoretical calculations beyond the mean-field approach, including the first QRPA calculations using the Gogny D1M parametrization for such heavy odd- N nuclei. The comparison points to the importance of accounting for the octupole vibrations for a proper understanding of the low-lying nuclear structure of some of the heaviest elements.

DOI: [10.1103/PhysRevC.97.054332](https://doi.org/10.1103/PhysRevC.97.054332)

I. INTRODUCTION

Unraveling the structure of transfermium nuclei ($Z \geq 100$) is a major challenge for both experimental and theoretical nuclear physics. Knowing the spacing and sequence of the unperturbed single-particle states is crucial for the understanding of the stability of these heaviest elements. Manifestations of collective particle motion largely define the position and ordering of nuclear excited states, often resulting in the rearrangement of levels as compared to the pure single-particle picture. Thus, through comparing the experimental results to mean-field or beyond-mean-field theoretical calculations, a better understanding of the collective effects and the role they play in the underlying nuclear structure can be achieved.

Recent experimental progress has demonstrated that $N = 150$ isotones have a low-lying 2^- excited state originating from an octupole vibration around the $N = 152$ and $Z = 100$ shell gaps [1]. In the odd $N = 151$ isotonic chain this phonon contributes to a low-lying $5/2^+$ level built on the $9/2^-$ ground state. As this $5/2^+$ state may only decay to the ground-state band, its decay is hindered, which allows us to easily isolate it based on its lifetime. These low-lying $5/2^+$ isomeric states in the $N = 151$ isotonic chain provide an invaluable opportunity to study the octupole transition strengths, and hence to probe the underlying structure of these heaviest elements.

As the decay of these isomers is highly converted, it is useful to combine standard γ -ray spectroscopy with internal conversion electron (ICE) measurements to extract more

complete spectroscopic data. In this paper we present the first combined γ -ICE measurements for ^{251}Fm . Moreover, this paper aims to trace the effect of the octupole vibration on the low-lying structure of the $N = 150$ and $N = 151$ isotones and to compare these experimental results to the quasiparticle random phase approximation (QRPA) calculations based on the Gogny D1M interaction and quasiparticle-phonon model (QPM) calculations based on the Woods-Saxon potential. This comparison is discussed in detail in Secs. V and VI.

II. EXPERIMENTAL DETAILS

Excited states in ^{251}Fm were populated via the α decay of ^{255}No produced in the $^{48}\text{Ca}(^{208}\text{Pb},n)^{255}\text{No}$ reaction directly, and in the $^{48}\text{Ca}(^{209}\text{Bi},2n)^{255}\text{Lr}$ reaction via a 26% electron capture branch from ^{255}Lr [2]. The cross sections of these reactions are 440 nb and 260 nb at midtarget beam energies of 220 MeV and 214 MeV [3], respectively. In 2004 and 2005, experiments with both ^{209}Bi and ^{208}Pb targets were performed using the VASSILISSA separator [4] with the GABRIELA spectrometer [5] at the focal plane. For these experiments GABRIELA consisted of a $58 \times 58 \text{ mm}^2$ position-sensitive implantation silicon detector with 16 resistive strips, a box of four silicon detectors, each divided into four pads, and seven Compton-suppressed 70% hyperpure coaxial germanium detectors: one behind the focal detector, coaxial to the beam and six in a ring around the focal plane. In the 2005 experiments one of the germanium detectors from the ring was missing, leading to the decrease of the total efficiency by a factor of ~ 1.08 . In the experiment performed in 2016 the $^{48}\text{Ca}(^{209}\text{Bi},2n)^{255}\text{Lr}$ reaction was used in an experiment with the SHELS

*kseniia.rezyunkina@kuleuven.be

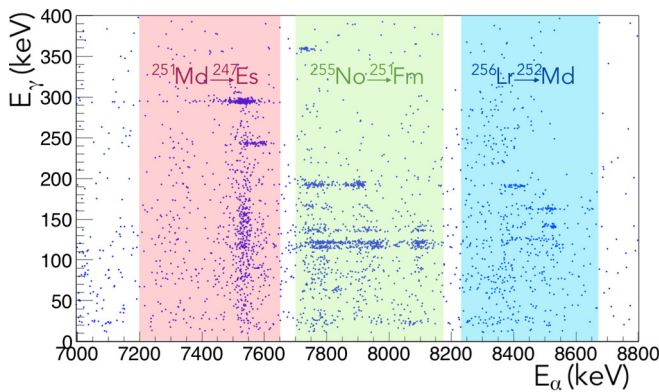


FIG. 1. α - γ coincidence plot for the 2016 data. The red band indicates the coincidences with ^{251}Md α decay, cyan band, ^{256}Lr α decay. The green band points to the coincidence of ^{251}Fm γ rays and ^{255}No α particles.

separator [6] (an upgrade of VASSILISSA) and the GABRIELA spectrometer. For this experiment GABRIELA consisted of a $100 \times 100 \text{ mm}^2$ double-sided silicon strip detector (DSSD) with 128×128 strips at the focal plane, surrounded by a box of eight DSSDs (two per side) with 16×16 strips each, a clover germanium detector consisting of four crystals behind the focal detector and four Compton-suppressed lateral 70% hyper-pure coaxial germanium detectors in a ring around the focal plane.

As the experimental campaigns of 2004 and 2005 were performed in practically identical conditions, the data from both years were treated as one data set. However, the 2016 setup was different from 2004 + 2005 in many aspects (thresholds, efficiency, number of strips and detectors, etc.). In addition there were technical problems with the readout electronics of the silicon box in 2016 leading to a significant decrease of its efficiency. Thus the data set from 2016 was treated separately.

The germanium detectors were calibrated with standard calibration sources (^{60}Co , ^{113}Sn , ^{152}Eu). The calibration of silicon detectors were performed in-beam with α and ICE

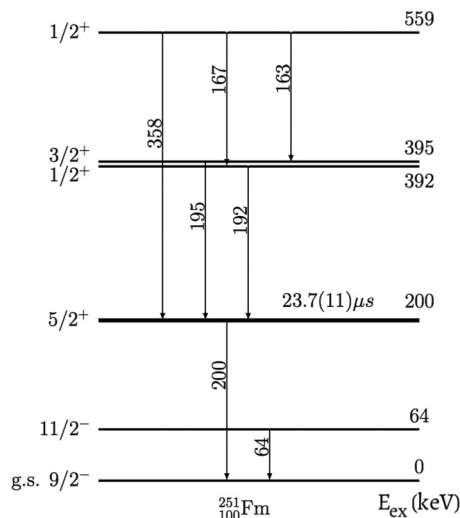


FIG. 2. A simplified level scheme depicting the observed transitions in ^{251}Fm populated in α decay of ^{255}No .

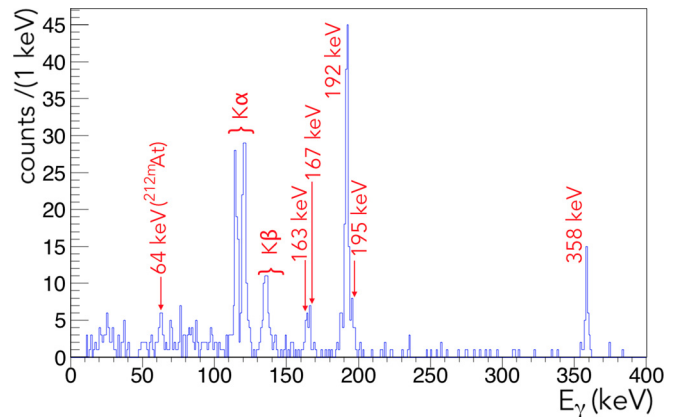


FIG. 3. The γ - and x rays coincident to the α decay of ^{255}No ($E_\alpha = 7700\text{--}7920 \text{ keV}$) from 2016 data.

decay lines of the products of the $^{48}\text{Ca}(^{164}\text{Dy}, 3\text{--}5n)^{207\text{--}9}\text{Rn}$ and, for 2004 + 2005 data, also the $^{48}\text{Ca}(^{174}\text{Yb}, 5\text{--}6n)^{216\text{--}17}\text{Th}$ reactions.

III. EXCITED STATES IN ^{251}Fm

Several other fermium nuclei such as ^{251}Md and ^{256}Lr were also populated during the experiments. The decay of the excited states in ^{251}Fm was thus isolated by tagging on the prompt and delayed α - γ and α -ICE correlations gated on the ^{255}No α decays between 7700 keV and 8160 keV (see Fig. 1). A total amount of ~ 11000 ^{255}No α particles were detected in the 2004 + 2005 data and ~ 21000 in the 2016 data.

The observed prompt and delayed transitions in ^{251}Fm are summarized in the level scheme in Fig. 2. These data are in agreement with the previous decay studies of ^{251}Fm [7,8] and are discussed in the following sections.

A. Prompt transitions

The internal conversion electrons seen in coincidence with the ^{255}No α decay mainly come from the $192 \text{ keV } 1/2^+ \rightarrow 5/2^+$ transition (see Fig. 2). The $1/2^+$ level is populated directly in the α decay as well as from the second $1/2^+$ level above it. In order to measure the conversion coefficients for the $1/2^+ \rightarrow 5/2^+$ transition, a gate on the α -particle energies

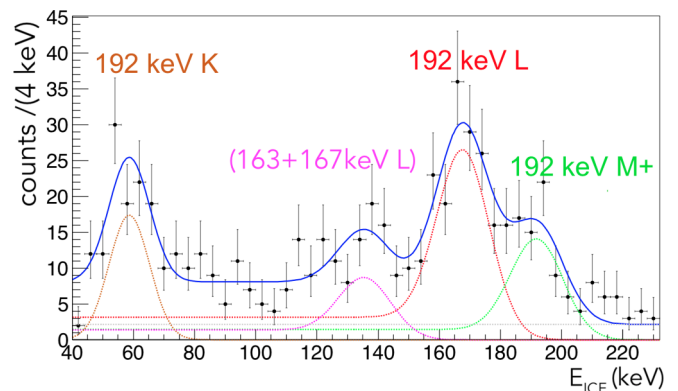


FIG. 4. The ICE coincident to the α decay of ^{255}No ($E_\alpha = 7700\text{--}7920 \text{ keV}$) from 2004 + 2005 data.

TABLE I. The number of K x rays expected from the observed γ -ray intensities (top part of the table) compared to the observed K x-ray intensities (bottom part), from 2016 data. The absolute intensities N_{xK} are calculated from the observed numbers of γ and x rays N , corresponding detection efficiencies ϵ and, for the γ rays, the ICC of the transitions.

E_γ	N	ϵ	Multipolarity	N_{xK}
163	12 ± 3	24%	$M1$	412 ± 113
167	9 ± 3	24%	$M1$	288 ± 96
192	121 ± 11	22%	$E2$	75 ± 7
195	20 ± 4	22%	$M1$	469 ± 103
358	23 ± 5	15.8%	$E2$	10 ± 2
TOT				1254 ± 181
K_α	247 ± 16	26.3%		939 ± 60
K_β	81 ± 9	25.5%		318 ± 35
TOT				1257 ± 70

between 7700 keV and 7920 keV, which incorporates all the transitions feeding the $1/2^+$ level, was applied. The α -gated γ -ray spectrum with this condition is given in Fig. 3; the α -gated ICE spectrum is given in Fig. 4. In the 2004+2005 data, 31(6) 192 keV γ rays are observed with a detection efficiency of 7.3%. In the 2016 data, there are 126(11) γ rays in the 192 keV peak with a 21.2% detection efficiency.

The internal conversion electrons from the 192 keV transition have the following energies: 50 keV, 167 keV, and 186 keV for K, L, and M conversion, respectively [9]. In the 2016 data, the K-conversion line mostly appears below the detection threshold, hence no data on K-conversion electrons can be extracted from this data set. The 163 keV and 167 keV transitions, both of which contribute to feeding of the $1/2^+$ level, are also converted. As the K-ICE of these transitions have energies of 21 keV and 25 keV, respectively, they appear below the energy threshold and cannot be detected. The L-ICE of both transitions cannot be resolved and appear in a peak of ~ 140 keV.

No significant contribution of the 358 keV transition to the prompt ICE spectrum is observed, leading to the conclusion that this transition is most likely of $E2$ nature. A weak 354 keV transition was observed in Ref. [7]. It was tentatively assigned as an $E1$ transition connecting a $7/2^+$ state at 354 keV excitation energy to the $9/2^-$ ground state. The conversion of

TABLE II. The energies E_{ICE} , detection efficiencies ϵ and intensities N of the prompt ICE transitions in ^{251}Fm from the experiments performed in 2004+2005 and 2016.

	E_{ICE} , keV	2004+2005		2016	
		ϵ	N	ϵ	N
K(192)	50	15.5%	50 ± 8		
L(192)	167	17.5%	79 ± 12	10.4%	76 ± 11
M+(192)	186	17.5%	40 ± 8	10.4%	34 ± 8
L(163+167)	~ 140	17%	21 ± 6	10.4%	20 ± 7

TABLE III. The comparison of the experimental internal conversion coefficients for the 192 keV transition from 2004+2005 and 2016 data compared to the theoretical $E2$ conversion coefficients.

	2004+2005	2016	$E2$ [9]
α_K	0.76(18)		0.139(2)
α_L	1.06(25)	1.23(21)	1.03(2)
α_M	0.54(15)	0.55(14)	0.293(5)
α_{tot}	2.36(35)		1.57(2)

this transition should not constitute any significant background to the rest of the observed ICE lines.

As the applied α -particle energy cut allows for the population of a number of excited states in ^{251}Fm , there might be some highly converted transitions contributing to the prompt ICE spectra that have not been seen in γ rays. In order to exclude such contributions, we have compared the observed K x-ray intensities to the number of K x rays expected from the observed γ -ray intensities. All transitions observed in γ rays were taken with the most likely (lowest possible) multiplicities. The results of this comparison are presented in Table I. As the expected number of K x rays agrees very well with the observations we may conclude that there is no other important K-conversion contribution to the ICE spectra that has not been taken into account in the present analysis.

In order to deduce the intensity of each ICE line, multicomponent fits were performed: each peak was approximated with a Gaussian skewed towards the low-energy side representing the full energy deposition by the ICE, plus an error function starting at the mean value of the Gaussian and going down to zero corresponding to the electrons backscattering from the detector. The ratio of the integrals of an error function and a Gaussian is related to the physical properties of the detector (thickness of the dead layer) and to the implantation depth of the evaporation residue, and thus remains the same for each ICE line. The fitted ICE intensities are given in Table II.

The internal conversion coefficients for the 192 keV transition deduced from the numbers of detected γ rays and ICE are given in Table III. These results are in agreement with the early measurements from Ref. [10] based on γ -ray spectroscopy and

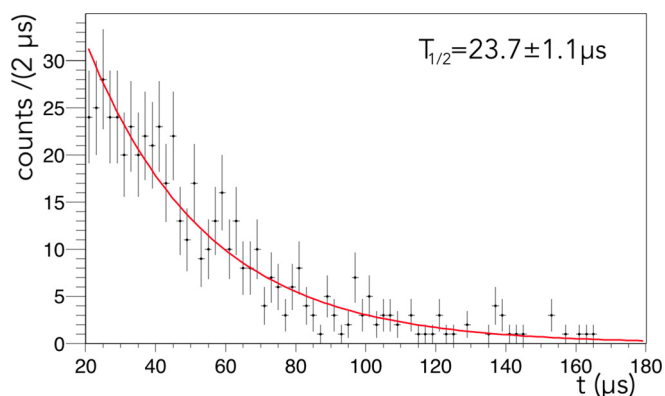


FIG. 5. Time distribution of the ICE emission from the $5/2^+$ isomeric state in ^{251}Fm and associated fit result (from the 2004+2005 data).

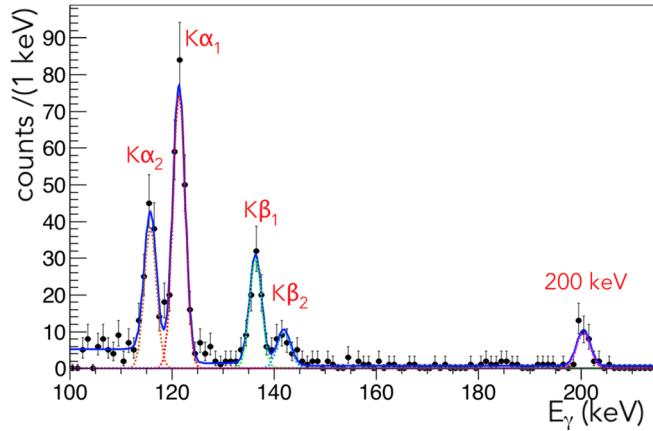


FIG. 6. Isomeric γ and x rays following the α decay of ^{255}No ($E_\alpha = 7700\text{--}8160$ keV) in the 2016 data.

allow us to confirm the $E2$ nature of this transition previously suggested in Ref. [7].

B. Decay of the isomer

The occurrence of an isomeric decay of a low-lying $5/2^+$ state to the $9/2^-$ ground state in ^{251}Fm was first reported in the early studies by Bemis *et al.* [10] and further confirmed in [7,8]. The half-life of the isomeric state was determined from the delayed α -ICE correlations in the 2004+2005 data. The half-life of the isomer determined through a single-component fit to the time distribution of the ICE emission is $23.7(11)$ μs (see Fig. 5). This result is in agreement with the previously reported values: $21(3)$ μs [8] and $21.1(19)$ μs [7].

In order to select the α decay branches contributing to the feeding of the $5/2^+$ isomeric state in ^{251}Fm , the correlations with α particles of 7700–8160 keV were selected. In order to exclude any random correlation background in the γ -ray spectra, the correlations within up to 50 μs from the α decay were taken. The γ - and x-ray spectrum of the decay of the isomer is given in Fig. 6. The intensities obtained from both data sets are given in Table IV.

The ICE spectra of the isomer are given in Fig. 7. The determined ICE intensities from both data sets are given in Table V. Due to the higher energy thresholds, only the L and M+ intensities were deduced from the 2016 data.

TABLE IV. Energies, corresponding detection efficiencies ϵ and measured intensities I of the γ and x rays from the isomeric transition in ^{251}Fm from the experiments performed in 2004+2005 and 2016.

E , keV	2004+2005		2016		
	ϵ	I	ϵ	I	
$K\alpha_2$	115	9.6%	44 \pm 9	26.5%	115 \pm 13
$K\alpha_1$	121	9.4%	98 \pm 10	26.2%	224 \pm 16
$K\beta_1$	136	8.8%	20 \pm 6	25.4%	90 \pm 10
$K\beta_2$	141	8.6%	23 \pm 6	24.9%	33 \pm 7
γ	200	7.1%	14 \pm 5	20.7%	33 \pm 6

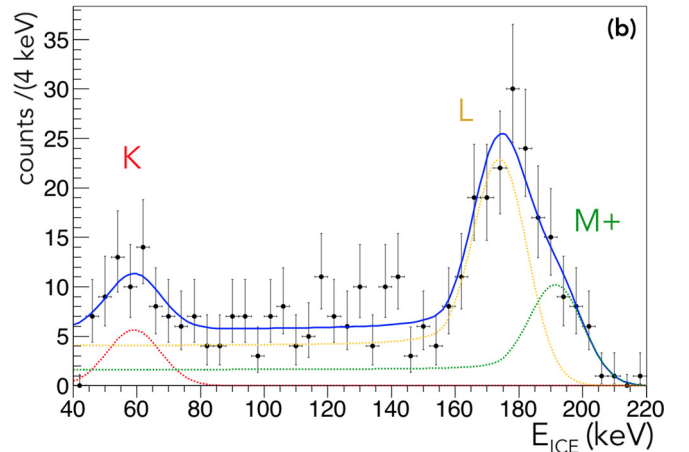
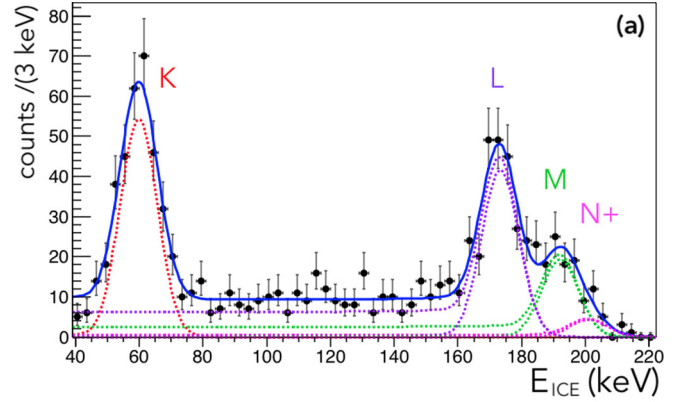


FIG. 7. The isomeric ICE following the α decay of ^{255}No ($E_\alpha = 7700\text{--}8160$ keV) 2004+2005 data (a) and 2016 data (b).

The internal conversion coefficients deduced in the present analysis are given in Table VI. These results are in a good agreement with the previously measured $\alpha_{KX} = 8.3(29)$ from [8]. The values clearly indicate the mixed $M2/E3$ nature of the 200 keV transition. The mixing ratios δ deduced from individual conversion coefficients are also given in Table VI. As the obtained confidence intervals for most of the measurements are large, the mean value of the mixing ratio (δ) cannot be assumed to be equal to $\delta(\alpha)$. Thus the mixing ratios were calculated

TABLE V. The energies, detection efficiencies and intensities of the ICE from the isomeric transition in ^{251}Fm from the experiments performed in 2004+2005 and 2016.

	E_{ICE}	2004+2005		2016	
		ϵ	N	ϵ	N
K	58 keV	15.5%	266 \pm 20		
L	173 keV	17.5%	280 \pm 31	10.4%	134 \pm 19
M(+) ^a	193 keV	17.5%	129 \pm 20	10.4%	61 \pm 16
N+	200 keV	17.5%	29 \pm 10		

^aIn the 2016 data, the N line could not be resolved, thus the M+ intensity is given.

TABLE VI. The conversion coefficients and the correspondingly deduced mixing ratios of the $5/2^+ \rightarrow 9/2^-$ isomeric transition in ^{251}Fm .

	2004+2005	2016	$M2$ [9]	$E3$ [9]	δ (2004+2005)	δ (2016)
α_K	8.8(31)		14.49(21)	0.227(4)	$0.2^{+0.43}_{-0.37}$	
α_{KX}	10.2(37)	11.5(23)			$0.2^{+0.44}_{-0.38}$	$0.2^{+0.23}_{-0.23}$
α_L	7.9(29)	8.1(19)	6.75(10)	11.05(16)	$1.2^{+1.1}_{-0.7}$	$1.2^{+0.9}_{-0.6}$
α_{tot}	21.2(75)		23.8(4)	15.93(23)	$0.2^{+0.16}_{-0.16}$	
α_K/α_L	1.07(16)		2.15(5)	0.0205(4)	$0.2^{+0.12}_{-0.12}$	

numerically through the convolutions of the corresponding probability density functions as described in Ref. [11].

The resulting average value of the mixing ratio is $\delta = 0.76^{+0.20}_{-0.19}$ (see Fig. 8). The obtained $M2/E3$ mixing and the measured lifetime of the 200 keV isomeric transition allow the corresponding Weisskopf single-particle estimates for the transition strengths in ^{251}Fm to be determined:

$$B(M2) = 3.0 \times 10^{-3} \pm 0.6 \times 10^{-3} \text{ W.u.}$$

$$B(E3) = 18 \pm 6 \text{ W.u.}$$

Evidence of two other delayed ICE lines at ~ 110 keV and ~ 130 keV was observed in both the 2004+2005 and the 2016 data sets. It could be interpreted as L and M conversion of the $5/2^+$ level decay to the $11/2^-$ level from the ground-state band, which was previously observed to be fed directly in the α decay of ^{255}No [7]. Such a transition should have the $E3$ multipolarity, and thus be highly converted ($\alpha_{\text{tot}}(E3) = 118.4(17)$ [9]), which would explain the absence of an observed γ line. However, due to the low statistics, no conclusive assignment can be made for the existence of this transition.

IV. SYSTEMATICS OF THE LOW-LYING $5/2^+$ STATE IN $N = 151$ ISOTONES

The assignment of the $9/2^-$ spin and parity to the ground state in ^{251}Fm comes from the systematics for the $N = 151$ isotones. This spin and parity assignment for the ground state was made through electron paramagnetic resonant spectroscopy in ^{247}Cm [12] and via laser spectroscopy in ^{253}No [13], as well as indirectly in ^{249}Cf α decaying to ^{245}Cm , which is known

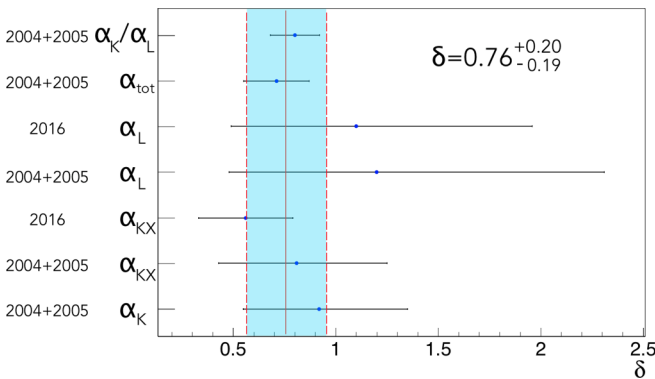


FIG. 8. The mixing ratios obtained through the different conversion coefficients measurements. The dashed blue area represents the mean confidence interval of δ .

[14] to have a $7/2^+[624]$ ground state. A schematic diagram of the proton and neutron orbitals active in this region is given in Fig. 9.

For the $N = 149$ isotones in this region the ground state is $7/2^+[624]$, and the first excited state is $5/2^+[622]$ [7]. $N = 147$ isotones have a $5/2^+[622]$ [16] ground state. Thereby the first excited single-particle state in $N = 151$ isotones that have one more occupied neutron orbital should be the $7/2^+[624]$ state. However, in ^{251}Fm a low-lying $5/2^+$ level is observed below the $7/2^+[624]$ at an excitation energy of 200 keV. The spin and parity of this level are deduced from the decay properties of the isomer: an $M2/E3$ multipolarity implies that the level should either have $5/2^+$ or $13/2^+$ spin and parity. As there is no $13/2^+$ orbital present in the region, and also as the α decay from the $1/2^+$ ground state in ^{255}No to a $13/2^+$ state would be very hindered, the low-lying state has to involve the $5/2^+[622]$ orbital. Similar behavior can be traced in the ^{247}Cm to ^{253}No $N = 151$ isotones, with the inversion of the $5/2^+$ and $7/2^+$ levels happening after ^{245}Pu (see Fig. 10). There is also recent experimental evidence of a low-lying isomer in ^{255}Rf [17], although a firm assignment is yet to be established.

V. INTERPRETATION

A. 2^- state in the $N = 150$ isotones

The very strong value of $B(E3) = 18(6)$ W.u. in ^{251}Fm indicates that for the low-lying structure of this nucleus large collective effects are at play. This in turn explains the low excitation energy of the $5/2^+$ state in ^{251}Fm .

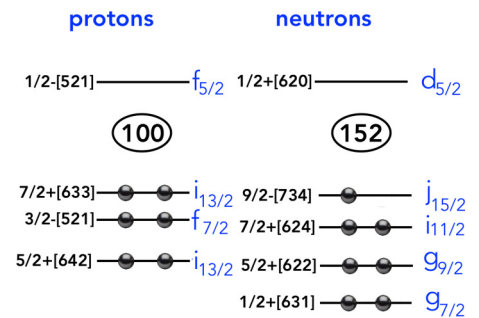


FIG. 9. A schematic diagram of the proton and neutron orbitals active around ^{251}Fm . The $Z = 100$ and $N = 152$ gaps come from the Woods-Saxon calculations (see, e.g., Ref. [15]). The orbitals and asymptotic Nilsson labels are indicated on the left in black, the spherical shell model labels are on the right in blue.

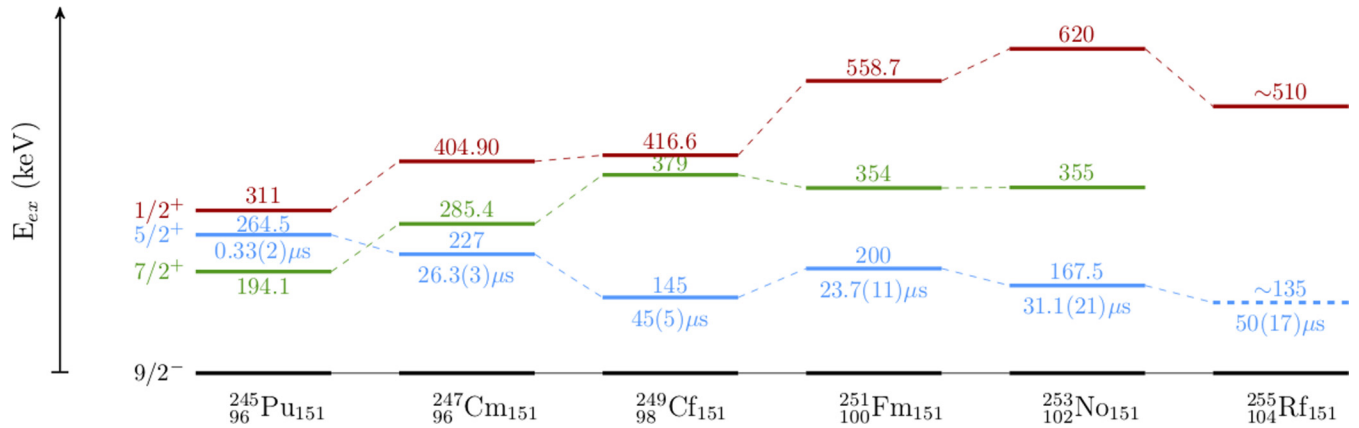


FIG. 10. Systematics of the excited states in $N = 151$ isotones, taken from Refs. [17–21] and this work.

The existence of this collective effect was first suggested by Yates *et al.* [22,23] who observed a $K^\pi = 2^-$ phonon built on the ^{246}Cm , ^{248}Cf , and ^{249}Cf ground states via transfer reactions. The proton and neutron content of the phonon was qualitatively studied in transfer reactions: it was demonstrated that the 2^- state in ^{250}Cf populated in the (α, t) [24] reaction must, as the ground state in ^{249}Bk , contain a proton component, while the 2^- state in ^{248}Cf produced in the (d, t) reaction should carry a neutron component from the ^{249}Cf ground state.

The octupole vibration mainly arises from the interplay of the levels coming from the $g_{9/2}$ and $j_{15/2}$ neutron shells having $\Delta j = \Delta l = 3$ (see Fig. 9). There is a similar occurrence on the proton side with $7/2^+$ [633] and $3/2^-$ [521] orbitals stemming from the proton shells $f_{7/2}$ and $i_{13/2}$ respectively. It turns out that the lowest octupole phonon has $K^\pi = 2^-$ [1,22]. This phonon yields a low-lying 2^- vibrational state in the even-even $N = 150$ isotonic chain from ^{246}Cm to ^{252}No . The systematics of the experimental 2^- energies is given in Fig. 11.

The 2^- phonon has not yet been observed in ^{254}Rf . However, the observation of an 893 keV γ ray in coincidence with a cascade of converted transitions reported by David *et al.* [25] might be the signature of the presence of this collective excitation. The 893 keV transition could be a transition connecting the 2^- band head to the first excited state of the ground-state rotational band and therefore correspond to the 799 keV line in ^{246}Cm [27], the 593 keV line in ^{248}Cf [22], the 834 keV line in ^{250}Fm [28], and 883 keV line in ^{252}No [1]. If the transition is $2^- \rightarrow 2^+$, the excitation energy of the 2^- state would be ~ 940 keV, as the 2^+ must be ~ 45 keV above the ground state. Such an estimate agrees well with the systematics (see Fig. 11). If the most intense transition is between the higher members of the 2^- and ground-state bands (e.g., in ^{252}No), the excitation energy is not easy to estimate.

In Fig. 11 the experimental measurements of the excitation energy of the 2^- state are compared to theoretical calculations. From the experimental values (traced in blue) it is clearly visible that the excitation energy of the 2^- level is almost

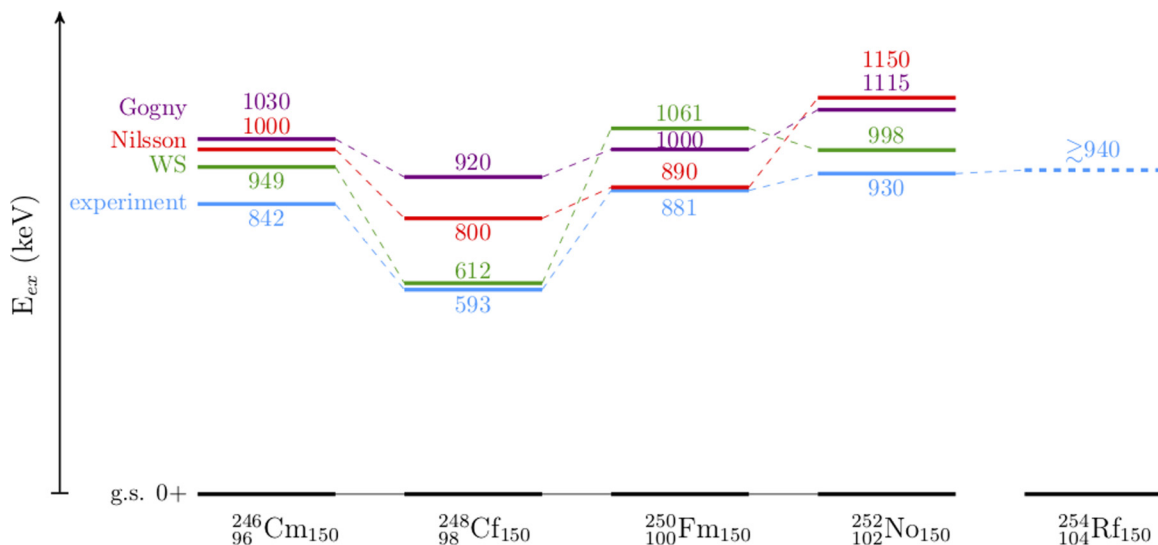


FIG. 11. Systematics of the $K^\pi = 2^-$ phonon excited state in $N = 150$ isotones. Experimental values (blue) taken from Refs. [1,25]; the QPM calculations with Nilsson potential [1] are given in red; present QRPA calculations with DIM parametrization of Gogny interaction are given in violet (the excitation energies have not been corrected for the rotational energy of the band heads); QPM calculations with the Woods-Saxon (WS) potential from Ref. [26] are given in green.

TABLE VII. Theoretical calculations for the 2^- vibrational state in $N = 150$ isotones. QRPA calculations from [1] with Nilsson potential; present QRPA calculations with the DIM parametrization of the Gogny interaction [33], π and ν are the proton and neutron content of the phonon respectively; QPM calculations with the Woods-Saxon potential from Refs. [26,34]. The experimental values are from Refs. [1,23].

	Experiment		Nilsson		Gogny DIM			Woods-Saxon	
	E^* , keV	$B(E3)$, W.u.	E^* , keV	E^* , keV	π , %	ν , %	$B(E3)$, W.u.	E^* , keV	$B(E3)$, W.u.
^{246}Cm	842	10.6	1000	1030	28	72	10.2	949	12.9
^{248}Cf	593		800	920	34	66	11.0	612	17.4
^{250}Fm	881		890	1000	28	72	10.0	1061	10.9
^{252}No	930		1150	1115	18	82	8.3	998	13.5

constant for $Z = 96-102$ with the exception of a noticeable kink in ^{248}Cf . In californium the proton single-particle states $7/2^+$ [633] and $3/2^-$ [521] are near the Fermi surface, and in ^{249}Bk [29] it is known that they are nearly degenerate. Thus, the proton collective component is more pronounced in ^{248}Cf than in other members of the $N = 150$ isotonic chain. This is evidence that there is no deformed shell gap at $Z = 98$, as predicted with the Gogny DIM parametrization. The same may also be concluded from the masses and from the excitation energies of the yrast 2^+ states in this region, which suggest the occurrence of a deformed shell gap at $Z = 100$ only, as given, e.g., in Ref. [15].

The comparison of various theoretical calculations for the 2^- collective state is given in Table VII. The QRPA calculations by Robinson *et al.* [1] are performed with the Nilsson potential within the theoretical framework described in Ref. [30]. The QPM calculations performed by Jolos *et al.* [26] were carried out with the Woods-Saxon potential. The present QRPA calculations were performed using the Hartree-Fock-Bogoliubov approximation with the Gogny DIM parametrization [31]. A detailed description of the QRPA calculations can be found in Ref. [32] for even-even nuclei and in Ref. [33] for odd nuclei. The QPM calculations yield a 2^- phonon with a major proton component peaking at $Z = 98$ with 62% two-quasiparticle-proton and 16% two-quasiparticle-neutron excitations [26]. However, the predictions of Gogny calculations favour the neutron component, with the proton content being maximal for ^{248}Cf : 66% two-quasiparticle-neutron and 34% two-quasiparticle-proton excitations. Moreover, since a proton deformed shell gap appears at $Z = 98$ with the Gogny

interaction, the dip in the excitation energy of the 2^- level at $Z = 98$ is not as pronounced in these calculations.

It is obvious from Fig. 11 that none of the theoretical calculations reproduce the experimental excitation energies. However, the absolute value of the excitation energy highly depends on the parametrization of the multipole-multipole interaction and a small shift in the parameters of the order of 2% may result in an energy shift of a few hundred keV [1]. In this respect the QPM calculations reproduce the behavior of the 2^- level more closely, despite the energy shift by ~ 200 keV.

B. $5/2^+$ state in the $N = 151$ isotones

In the $N = 151$ isotonic chain the 2^- phonon built upon the single-particle $9/2^-$ ground state yields a vibrational $5/2^+_{\text{vib}}$ state, which in turn interacts with the single-particle $5/2^+$ level thus yielding two mixed levels: one carrying more of a single-particle component and the other, a larger phonon component. Due to the collective octupole admixture, the $5/2^+$ level gets pushed down in energy, becoming the first excited state in the $N = 151$ isotones in curium and above (see Fig. 10). This phonon admixture also yields the large value of octupole transition strength observed in this work.

The same pattern is observed in doubly magic ^{208}Pb region, where a similar configuration of $g9/2$ and $j15/2$ neutron shells gives rise to the existence of a 3^- octupole phonon, which turns out to be the first excited state in ^{208}Pb [35]. In ^{209}Pb the phonon built upon the $9/2^+$ ground state yields a $15/2^-$ level, which mixes and repels with the single-particle $15/2^-$ (see Fig. 12). The higher-lying $5/2^+$ level carrying a larger fraction of the

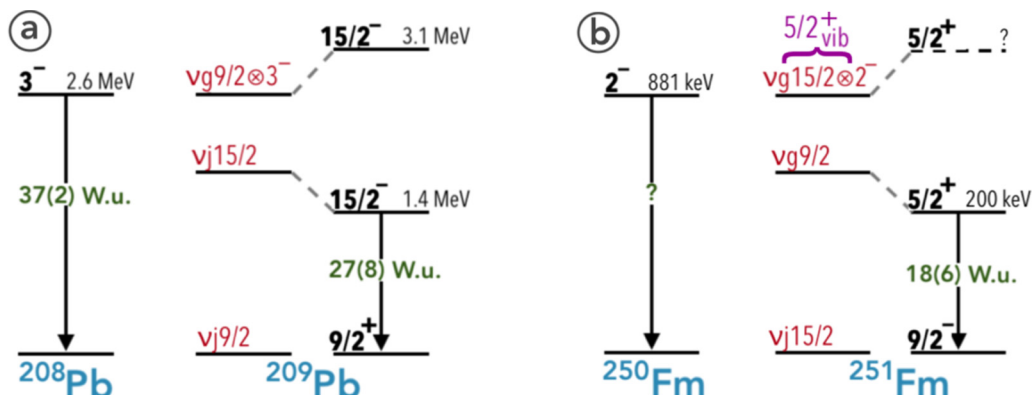


FIG. 12. (a) The $K^\pi = 3^-$ phonon in ^{208}Pb and ^{209}Pb [35]; (b) the $K^\pi = 2^-$ phonon in ^{250}Fm and ^{251}Fm .

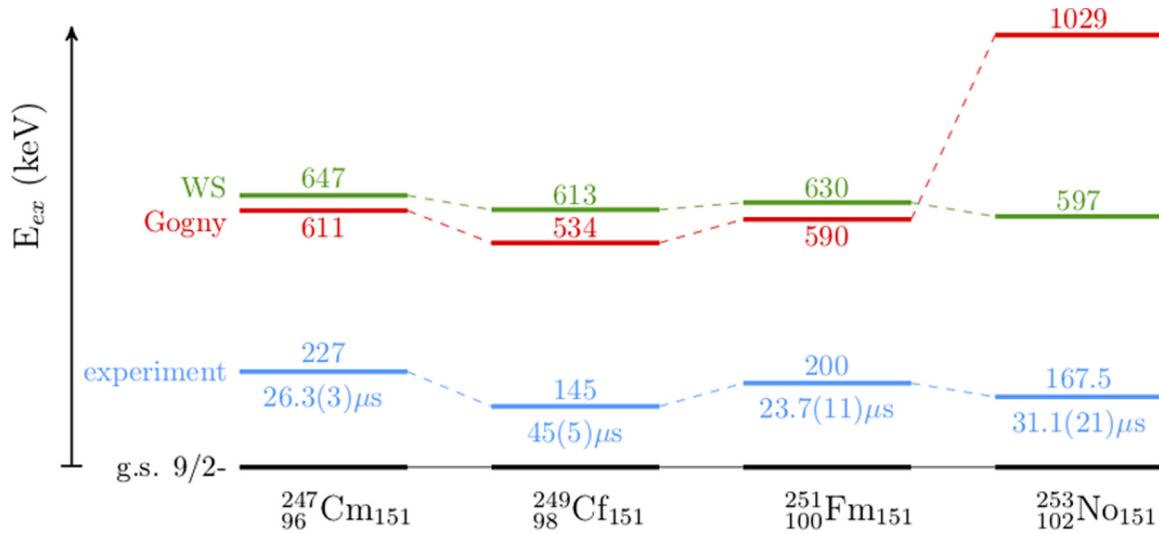


FIG. 13. Systematics of the $5/2^+$ level in $N = 151$ isotones. Experimental values (blue) taken from Refs. [18–21] and this work; present QRPA DIM calculations for the $5/2^+_{\text{vib}}$ state are plotted in red; QPM calculations with Woods-Saxon potential from Ref. [34] are given in green.

$9/2^- \otimes 2^-$ component has not been observed in any of the $N = 151$ isotones, probably due to the low α decay feeding.

In Fig. 13 the experimental $5/2^+$ excitation energies are compared to the theoretical calculations. The excitation energy calculated with QRPA in present work using the Gogny DIM interaction follows the trend of the experimental values for $Z = 96$ – 100 , but fails at $Z = 102$. This is due to the incompleteness of the basis of relevant two-quasiparticle excitations in the case of ^{253}No . Indeed, in going from ^{251}Fm to ^{253}No , the occupation of the $9/2^-$ orbital changes significantly resulting in a reduction of possible excitations due to the blocking scheme used in the calculations. Allowing for hole excitations in the $9/2^-$ orbital is estimated to result in a $5/2^+$ state below the one calculated for ^{251}Fm , in agreement with the experimental data. The octupole transition strengths were also calculated, though they do not account for mixing with quasiparticle states and thus only provide an upper limit for the strengths that can be measured experimentally. Nevertheless the predicted $B(E3)_{\text{theor}}$ (see Table VIII) are of the same order or smaller than the experimental values and therefore require further investigation.

According to the QPM calculations (see Table IX), the separation energy between the two $5/2^+$ states is of the order

TABLE VIII. Results of the present QRPA calculations with DIM for the $5/2^+_{\text{vib}}$ state in $N = 151$ isotones. π and ν are the proton and neutron content of the phonon respectively. The predicted excitation energy E_{th}^* is given for the $K^\pi = 2^-$ phonon excitation built on the $9/2^-$ ground state without taking into account the mixing with the single-particle $5/2^+$ excitation. The excitation energies and strengths are from Refs. [19–21] and this work.

	E_{exp}^* , keV	$B(E3)_{\text{exp}}$	E_{th}^* , keV	π , %	ν , %	$B(E3)_{\text{th}}$
^{247}Cm	227	7.3(21) W.u.	611	15	85	9.8 W.u.
^{249}Cf	145	10(4) W.u.	534	18	82	11.1 W.u.
^{251}Fm	200	18(6) W.u.	590	13	87	9.2 W.u.
^{253}No	168	13(8) W.u.	(1029)			

of 400 keV and the phonon content of the lower $5/2^+$ is $\sim 10\%$, with the exception of ^{249}Cf , where it peaks at 18%. This value can be compared to 29(5)% phonon content extracted from $^{249}\text{Cf}(d, d')$ data [22].

As it was mentioned before, though the predicted excitation energies are ~ 400 keV higher than the experimental ones, a small change of the parameters may result in a significant variation of these values, and thus the general trend is more important. These calculations reproduce the general evolution of the excitation energy of the $5/2^+$ level observed experimentally (see Fig. 10), though the predicted variation of the excitation energy and phonon content for ^{249}Cf is less strong than the experimentally observed behaviors. A possible explanation is that the $5/2^+[622]$ single-particle level should lie closer to its pseudo-spin-partner $7/2^+[624]$ level than it appears from the Woods-Saxon potential, which should result in a more accurate reproduction of the excitation energy pattern along both isotonic chains.

VI. CONCLUSION

Combined γ and ICE spectroscopy of the decay of excited states in ^{251}Fm populated by α decay of ^{255}No allowed the measurement of conversion coefficients for the 192 keV and

TABLE IX. Results of QPM calculations with the Woods-Saxon potential [34] for the $5/2^+$ states in $N = 151$ isotones.

	E_{exp}^* , keV	E^* , keV	Structure
^{247}Cm	227	647	$5/2^+[622]85\% + 9/2^- [734] \otimes 2^- 10\%$
	?	1096	$9/2^- [734] \otimes 2^- 86\% + 5/2^+[622]10\%$
^{249}Cf	145	613	$5/2^+[622]77\% + 9/2^- [734] \otimes 2^- 18\%$
	?	982	$9/2^- [734] \otimes 2^- 79\% + 5/2^+[622]18\%$
^{251}Fm	200	630	$5/2^+[622]88\% + 9/2^- [734] \otimes 2^- 8\%$
	?	1099	$9/2^- [734] \otimes 2^- 87\% + 5/2^+[622]9\%$
^{253}No	168	597	$5/2^+[622]89\% + 9/2^- [734] \otimes 2^- 7\%$
	?	1099	$9/2^- [734] \otimes 2^- 86\% + 5/2^+[622]8\%$

200 keV electromagnetic transitions. The evidence of a new $5/2^+ \rightarrow 11/2^-$ transition in the decay of the $5/2^+$ isomer has been observed in the ICE spectra. The $M2/E3$ mixing ratio for the decay of the $5/2^+$ isomer to the ground state was measured to be $\delta = 0.2^{+0.20}_{-0.19}$. The electric octupole and magnetic quadrupole transition strengths equal to $18(6)$ W.u. and $3.0(6) \times 10^{-3}$ W.u. respectively, have been extracted.

Particle-phonon mixing in the $5/2^+$ state in $N = 151$ isotones is responsible for the enhanced $B(E3)$ strength of its de-excitation, as well as for the lowering of its excitation energy. The effect of this low-lying octupole phonon is traced in the experimental data along the $N = 151$ isotonic chain. The experimental data are compared to the results from consistent QRPA calculations with the Gogny interaction and QPM calculations with the Woods-Saxon potential, as well as results from QRPA based on the Nilsson potential for the $N = 150$ isotones. This comparison suggests that the two-quasiparticle basis of the present QRPA Gogny DIM calculations should be enlarged in order to include single-particle excitations in addition to the vibrational ones for the odd systems.

The particle-phonon interaction plays an important role in the structure of nuclei in the region near the $Z = 100$ and $N = 152$ shell gaps. It is also possible that the presence of

octupole correlations is responsible for other phenomena, such as lowering of the first 2^+ energies and masses in $Z = 98$ isotopes [36]. Further advances on the theoretical side are needed for a description of the properties of low-lying states in the region. Care needs to be taken when comparing the experimental data to the predicted trends of single-particle excitations in the transfermium region, as the excitation energies and transition strengths may be highly perturbed by collective correlations. Beyond-mean-field calculations are required in order to understand the underlying structure of the heaviest nuclei.

ACKNOWLEDGMENTS

The GABRIELA project is jointly funded by CNRS (France) and JINR (Russia). The modernization of the separator SHELS and spectrometer GABRIELA was financed by the ANR (Contracts No. ANR-06-BLAN-0034-01 and No. ANR-12-BS05-0013-02, respectively) and by RFBR (Grants No. 17-02-00867 and No. 18-52-15004). The authors would like to thank the French-UK Loan Pool for providing the coaxial germanium detectors, and R. V. Jolos and L. A. Malov for the fruitful discussions upon the QPM calculations.

-
- [1] A. P. Robinson, T. L. Khoo, I. Ahmad, S. K. Tandel, F. G. Kondev, T. Nakatsukasa, D. Seweryniak, M. Asai, B. B. Back, M. P. Carpenter, P. Chowdhury, C. N. Davids, S. Eeckhaudt, J. P. Greene, P. T. Greenlees, S. Gros, A. Heinz, R. D. Herzberg, R. V. F. Janssens, G. D. Jones, T. Lauritsen, C. J. Lister, D. Peterson, J. Qian, U. S. Tandel, X. Wang, and S. Zhu, *Phys. Rev. C* **78**, 034308 (2008).
- [2] K. Hauschild, A. Lopez-Martens, A. V. Yeremin, O. Dorvaux, S. Antalic, A. V. Belozherov, C. Briancon, M. L. Chelnokov, V. I. Chepigin, D. Curien, B. Gall, A. Gorgen, V. A. Gorshkov, M. Guttormsen, F. Hanappe, A. P. Kabachenko, F. Khalfallah, A. C. Larsen, O. N. Malyshev, A. Minkova, A. G. Popeko, M. Rousseau, N. Rowley, S. Saro, A. V. Shutov, S. Siem, L. Stuttge, A. I. Svirikhin, N. U. H. Syed, C. Theisen, and M. Venhart, *Phys. Rev. C* **78**, 021302 (2008).
- [3] H. W. Gäggeler *et al.*, *Nucl. Phys. A* **502**, 561 (1989).
- [4] A. V. Yeremin *et al.*, *Nucl. Instrum. Methods A* **350**, 608 (1994).
- [5] K. Hauschild *et al.*, *Nucl. Instrum. Methods A* **560**, 388 (2006).
- [6] A. V. Yeremin *et al.*, *Phys. Part. Nucei Lett.* **12**, 35 (2015).
- [7] M. Asai, *Phys. Rev. C* **83**, 014315 (2011).
- [8] F. P. Hessberger *et al.*, *Eur. Phys. J. A* **29**, 165 (2006).
- [9] BrIcc v2.3S, Conversion Coefficient Calculator, <http://bricc.anu.edu.au>.
- [10] C. E. Bemis, Jr. *et al.*, Report ORNL **4708**, 62 (1971).
- [11] K. Rezyunkina *et al.*, *Nucl. Instrum. Methods A* **844**, 96 (2017).
- [12] M. M. Abraham *et al.*, *Phys. Lett. A* **44**, 527 (1973).
- [13] M. Laatiaoui *et al.*, *Nature (London)* **538**, 495 (2016).
- [14] A. MacDonald *et al.*, *Nucl. Data Sheets* **114**, 397 (2013).
- [15] R. R. Chasman *et al.*, *Rev. Mod. Phys.* **49**, 833 (1977).
- [16] R.-D. Herzberg and P. T. Greenlees, *Prog. Part. Nucl. Phys.* **61**, 674 (2008).
- [17] S. Antalic *et al.*, *Eur. Phys. J. A* **51**, 41 (2015).
- [18] E. Browne and J. K. Tuli, *Nucl. Data Sheets* **112**, 447 (2011).
- [19] C. D. Nesaraja, *Nucl. Data Sheets* **125**, 395 (2015).
- [20] K. Abusaleem, *Nucl. Data Sheets* **112**, 2129 (2011).
- [21] A. Lopez-Martens *et al.*, *Eur. Phys. J. A* **32**, 245 (2007).
- [22] S. W. Yates *et al.*, *Phys. Rev. C* **12**, 442 (1975).
- [23] S. W. Yates *et al.*, *Phys. Rev. C* **12**, 795 (1975).
- [24] S. W. Yates *et al.*, *Phys. Rev. Lett.* **36**, 1125 (1976).
- [25] H. M. David, J. Chen, D. Seweryniak, F. G. Kondev, J. M. Gates, K. E. Gregorich, I. Ahmad, M. Albers, M. Alcorta, B. B. Back, B. Baartman, P. F. Bertone, L. A. Bernstein, C. M. Campbell, M. P. Carpenter, C. J. Chiara, R. M. Clark, M. Cromaz, D. T. Doherty, G. D. Dracoulis, N. E. Esker, P. Fallon, O. R. Gothe, J. P. Greene, P. T. Greenlees, D. J. Hartley, K. Hauschild, C. R. Hoffman, S. S. Hota, R. V. F. Janssens, T. L. Khoo, J. Konki, J. T. Kwarsick, T. Lauritsen, A. O. Macchiavelli, P. R. Mudder, C. Nair, Y. Qiu, J. Rissanen, A. M. Rogers, P. Ruotsalainen, G. Savard, S. Stolze, A. Wiens, and S. Zhu, *Phys. Rev. Lett.* **115**, 132502 (2015).
- [26] R. V. Jolos *et al.*, *J. Phys. G: Nucl. Part. Phys.* **38**, 115103 (2011).
- [27] E. Browne *et al.*, *Nucl. Data Sheets* **112**, 1833 (2011).
- [28] P. T. Greenlees, R.-D. Herzberg, S. Ketelhut, P. A. Butler, P. Chowdhury, T. Grahn, C. Gray-Jones, G. D. Jones, P. Jones, R. Julin, S. Juutinen, T. L. Khoo, M. Leino, S. Moon, M. Nyman, J. Pakarinen, P. Rahkila, D. Rostron, J. Saren, C. Scholey, J. Sorri, S. K. Tandel, J. Uusitalo, and M. Venhart, *Phys. Rev. C* **78**, 021303(R) (2008).
- [29] D. Seweryniak *et al.*, *Nucl. Phys. A* **834**, 357c (2010).
- [30] T. Nakatsukasa, K. Matsuyanagi, S. Mizutori, and Y. R. Shimizu, *Phys. Rev. C* **53**, 2213 (1996).
- [31] S. Goriely, S. Hilaire, M. Girod, and S. Peru, *Phys. Rev. Lett.* **102**, 242501 (2009).
- [32] S. Péru and M. Martini, *Eur. Phys. J. A* **50**, 88 (2014).
- [33] I. Deloncle *et al.*, *Eur. Phys. J. A* **53**, 170 (2017).
- [34] R. V. Jolos and L. A. Malov (private communication).
- [35] P. Kleinheinz, *Phys. Scr.* **24**(1B), 236 (1981).
- [36] Ch. Theisen *et al.*, *Nucl. Phys. A* **944**, 333 (2015).